

ROLE OF NEURAL NETWORKS IN THE SEARCH OF THE HIGGS BOSON AT LHC

T. Maggipinto^a, G. Nardulli^{a,b}

^a *Dipartimento di Fisica, Università di Bari, Italy*

^b *Istituto Nazionale di Fisica Nucleare, Sez. di Bari, Italy*

S. Dusini^{c,d}, F. Ferrari^{c,f}, I. Lazzizzera^{c,d}, A. Sidoti^{c,d},

A. Sartori^{d,e}, G.P. Tecchiolli^{d,e}

^c *Dipartimento di Fisica, Università di Trento, Italy*

^d *Istituto Nazionale di Fisica Nucleare, Gruppo Coll. di Trento, Sez. di Padova, Italy*

^e *Istituto per la Ricerca Scientifica e Tecnologica, Trento, Italy*

^f *LPTHE, Universitès Paris VI - Paris VII, Paris, France*

BARI-TH/268-97

May 1997

ABSTRACT

We show that neural network classifiers can be helpful to discriminate Higgs production from background at LHC in the Higgs mass range $M_H \sim 200\text{GeV}$. We employ a common feed-forward neural network trained by the backpropagation algorithm for off-line analysis and the neural chip TOTEM, trained by the Reactive Tabu Search algorithm, which could be used for on-line analysis.

1 Introduction

The main purpose of the future Large Hadron Collider (LHC) at CERN is the search for the Higgs boson H , the only particle predicted by the Standard Model of the electroweak interactions that has not been discovered yet. The discovery of the Higgs particle would be of paramount importance in confirming the peculiar feature of the electroweak vacuum embodied in the spontaneous breaking of the $SU(2)_L \times U(1)$ electroweak symmetry; on the other hand, its absence from the physical spectrum would certainly pave the way for exciting new physics, be it in the form of supersymmetry, or theories with a strongly interacting Higgs sector [1] or something else.

The big theoretical and experimental effort that will be provided in the next few years is strongly motivated by the relevance of the stake, but also because, as the Standard Model predicts and detailed studies have confirmed [2], the signal, i.e. events characterized by the production of the Higgs boson, will be overwhelmed by background events, with multi-hadron production induced by strong interactions of quark and gluons. For this reason, a crucial step in the implementation of the LHC programme will be provided by data analysis, which will be asked to disentangle Higgs events from huge background. It is not our aim to review here the actual experimental set-up of the LHC experiments, nor to examine the performances of LHC detectors: the purpose of this letter is simply to suggest that part of the task to extract the signal from the noise could be supplied by Artificial Neural Networks (ANN)¹

The role of ANN in high energy physics experiments has been stressed in a number of papers and we refer the interested reader to the existing literature [4, 5, 6, 7, 8, 9, 10]; in general, when compared with traditional methods of statistical discrimination, they offer the advantage of possible on-line implementation and often better results in terms of purity and efficiency [11]. These latter features have been observed already in preliminary studies on the use of ANN for Higgs search at LHC [7]. The present analysis differs from these studies for two reasons:

- i) we adopt a more appropriate choice of the input variables;
- ii) we make a comparison between two implementations of ANN in the feed-forward architecture; namely, a simulated neural network trained by the usual backpropagation algorithm [12] is compared to a hardware realization of a low-precision-weight Multi-Layer Perceptron (MLP), the neurochip TOTEM [13], whose training-by-example task is accomplished by a derivative free *combinatorial optimization* algorithm called *Reactive Tabu Search* (RTS) [14, 15].

A detailed presentation of the two NN will be given in Sections 2 and 3. Here we conclude this introduction by stressing the limits and some of the general features of our analysis.

First of all we do not investigate the whole expected Higgs mass (M_H) range. From LEP data a lower bound for the Higgs mass is known: $M_H \gtrsim 60$ GeV [16]. Theoretical arguments based on unitarity or on the applicability of the perturbation theory indicate that M_H should not be larger than $\simeq 800$ GeV [17]; as for the analysis based on studies of radiative corrections, they appear still inconclusive, due to the weak dependence of these effects on M_H . Since we mainly wish to present some case studies, rather than to make

¹for a general introduction to ANN see [3].

an extensive review, we limit our analysis to the mass values of $M_H = 150$ and 200 GeV. In a range around these Higgs mass values the preferred decay channel, as indicated by previous studies [2, 7], is the following one:

$$p p \rightarrow H X \rightarrow 4\mu X . \quad (1.1)$$

For rather larger Higgs masses (≥ 400 GeV) the events (1.1) would be clearly distinguishable from the peak in the four-muon invariant mass. In our case, however, the signal should be overwhelmed by two main sources of background, namely the $t\bar{t}$ production:

$$p p \rightarrow t \bar{t} X \rightarrow \mu^+ \mu^- \mu^+ \mu^- X' , \quad (1.2)$$

with the 4 muons arising from semileptonic decays of the top and antitop, and the $Zb\bar{b}$ production:

$$p p \rightarrow Z b \bar{b} X \rightarrow \mu^+ \mu^- \mu^+ \mu^- X' , \quad (1.3)$$

with a muon pair arising from Z^0 decay and the other one from semileptonic b and \bar{b} decays. It should be observed that, due to the actual value of the top quark mass ($M_t = 175 \pm 12$ GeV [18]), the processes (1.2) and (1.3) have comparable cross sections; for their calculation we rely in this paper on the Pythia *Montecarlo* code [19]. At the LHC energy ($\sqrt{s} = 14$ TeV) one has²:

$$\sigma(pp \rightarrow t\bar{t}X \rightarrow \mu^+ \mu^- \mu^+ \mu^- X') = 7.8 \times 10^{-9} mb , \quad (1.4)$$

$$\sigma(pp \rightarrow Z^0 b\bar{b}X \rightarrow \mu^+ \mu^- \mu^+ \mu^- X') = 6.0 \times 10^{-9} mb . \quad (1.5)$$

These figures should be compared to the computed cross section for Higgs production and subsequent decay into four muons:

$$\sigma(pp \rightarrow H X \rightarrow ZZ^* X \rightarrow \mu^+ \mu^- \mu^+ \mu^- X) = 1.2 \times 10^{-12} mb \quad (1.6)$$

for $M_H = 150$ GeV;

$$\sigma(pp \rightarrow H X \rightarrow ZZ X \rightarrow \mu^+ \mu^- \mu^+ \mu^- X) = 2.8 \times 10^{-12} mb \quad (1.7)$$

for $M_H = 200$ GeV. The main difference between the two cases is that for $M_H = 200$ GeV the two Z s are real, while for $M_H = 150$ GeV only one is real, the other being virtual. As a consequence, in the latter case the constraint $M_{\mu\mu} = M_Z$ does not hold for one of the $\mu^+ \mu^-$ pairs.

For the use of ANNs in high energy physics a crucial point is the choice of sensible physical observables. On the base of previous studies [2, 7] the four final muons are ordered according to their energy, and the following 10 variables X_1, \dots, X_{10} are introduced:

$X_1 - X_4$: the transverse momentum of the four muons. The distributions of these variables for background events, as simulated by the Pythia *Montecarlo*, show a maximum close to zero for those muons coming from quark fragmentation, while the signal distributions show a peak around $25 - 50$ GeV; a similar distribution is found for the two muons deriving from Z decay in the $Zb\bar{b}$ background events;

²We notice that in some previous studies, performed before the discovery of the top quark, smaller values of M_t , e.g. 130 GeV, were in general adopted, which resulted in a higher cross section for the process (1.2) and a negligible one, in comparison, for the process (1.3).

$X_5 - X_8$: the invariant masses of the four different $\mu^+\mu^-$ pairs. For $M_Z < M_H < 2M_Z$, two of the distributions for the signal events show a peak around the Z^0 mass, that is absent for the background. The peaks arise from muons coming from the real Z^0 decay; they are two since the ordering based on the energy mixes in part the events from the two Z^0 . For $M_H \geq 2M_Z$, of course, all the four distributions exhibit the Z^0 mass peak;

X_9 : the four muons invariant mass;

X_{10} : the hadron multiplicity related to hard jets.

A comment on the variable X_{10} is in order. We expect that hadrons generated by hard parton scattering are more copiously produced by the process (1.3) and especially (1.2) as compared to (1.1). However such a peculiar feature of the events (1.1) is hidden in the huge number (typically several hundreds at the LHC energy) of hadrons produced by the hadronization of the two beam jets. The remnants of the two beams disintegration could be eliminated in the LHC experimental conditions by appropriate cuts in the angular variables, but in our simulations we choose to pre-process the data by the so called k_\perp clustering algorithm [20, 21]. This algorithm consists in general of two steps. In the first step one compares

$$d_{ij} = 2 \min\{E_{Ti}^2, E_{Tj}^2\} \sqrt{(\eta_i - \eta_j)^2 + (\phi_i - \phi_j)^2} \quad (1.8)$$

and

$$d_{iB} = E_{Ti}^2, \quad (1.9)$$

where E_{Ti} is the transverse energy of the i -th particle with respect to the beam direction, η_i is its pseudorapidity and ϕ_i is the azimuth angle with respect to the beam axis: a final state particle i is attributed to the beam remnants (beam jet) if d_{iB} is smaller than d_{ij} , otherwise it is attributed to a hard jet. In the second step, which is not of interest here, the particles belonging to hard jets are divided into different clusters³. After the application of the k_\perp algorithm and the removal of the hadrons belonging to the beam jets, the remaining hadron multiplicity is called by us X_{10} . The relevance of the variable X_{10} can be seen from Fig. 1, where we compare its distribution relative to the processes (1.1), (1.2) and (1.3).

Having defined the input variables, we now discuss the analyses performed on the Montecarlo data using the two neural networks.

2 Analysis by simulated ANN trained through the backpropagation algorithm

First we discuss the results obtained using a simulated net in the most common architecture adopted in high energy applications, i.e. the *feed-forward* MLP, trained through the "classical" backpropagation algorithm. The net is composed of one input layer with 10 neurons X_j , one hidden layer with 21 neurons z_j and one output unit y .

³For another application of k_\perp algorithm in the context of ANN studies of high energy physics experiments see [22].

The physical observables introduced above, once normalized to the interval $[-1, 1]$, become the inputs X_j ($j = 1, \dots, 10$) of the NN classifier. Each pattern-event p consists of the array X_j of the input variables (features) and the value y of the output neuron ($y = 1$ for the signal, i.e. the Higgs production, and $y = 0$ for the background). The patterns have been divided into two sets, the training set, used by the network to learn, and the testing set, used to evaluate subsequently its performance.

As already mentioned, our simulations have been obtained by the Pythia Montecarlo Code[19]. We have treated the case of two possible values for the mass of the Higgs particle: one below $2M_Z$ i.e. 150 GeV, and one just above, i.e. 200 GeV. For each of these mass values the training data set consisted of $N = 2000$ signal events, 2000 $t\bar{t}$ and 2000 $Zb\bar{b}$ events, while the testing data set consisted of 2000 $pp \rightarrow HX \rightarrow 4\mu X$ signal events, 5.6×10^6 $t\bar{t}$ and 4.2×10^6 $Zb\bar{b}$ background events for the case $M_H = 200$ GeV. The data in the training sets were all different from those in the testing sets.

As usual, the performance of the network has been evaluated by introducing two variables: the purity (P) and the efficiency (η) defined as follows:

$$P = \frac{N_H^a}{N_H^a + N_B^a} \quad (2.1)$$

and

$$\eta = \frac{N_H^a}{N_H} \quad (2.2)$$

where N_H is the total number of Higgs events in the testing sample, N_H^a is the total number of the accepted (i.e. correctly identified) Higgs events and N_B^a is the total number of the accepted background events, i.e. events that are incorrectly identified as Higgs events.

One can increase the purity decreasing the efficiency by introducing a threshold parameter $l \in [0, 1]$ as follows. The range of values of the output neuron $y^{(p)}$ in the testing phase is divided into the subintervals: $I_1 = [0, 1 - l]$ and $I_2 =]1 - l, 1]$, so that if $y^{(p)} \in I_1$ (respectively $y^{(p)} \in I_2$) the event is classified as background (respectively: signal).

Our results are reported in Fig. 2 (dots); it shows that in the case of $M_H = 200$ GeV one can reach appreciable values of purity. The situation is less favorable in the case of $M_H = 150$ GeV, when, due to the virtuality of one of the two Z , the reduction of efficiency is relevant.

3 Analysis using the RTS training algorithm as implemented on the neurochip TOTEM

One of the purposes of the present work is to contribute to clarify the possibility of using neural network classifiers in time-critical operations, like the fast triggering required in some high energy experiments, without loosing high quality performances. The neurochip TOTEM, has been conceived to implement Multi-Layer Perceptrons in the *feed-forward* architecture on the basis of a simple and fast computational structure [13]. This is achieved escaping the necessity of derivative calculations, turning the task of training-by-examples into a *combinatorial optimization* problem, whose solution is searched then by means of the *Reactive Tabu Search* method [14, 15]. Differently from the derivative-based back-propagation algorithms, RTS thus allows simple and low precision computation, using

only up to 8 bits for the synaptic weights and 16 bits to represent the feature parameters⁴: this is indeed the basis of the simple and fast computational structure said above. TOTEM can be set to different *feed-forward* MLP architectures and for the present work it has been given exactly the same 10-21-1 architecture as the network described in the preceding section. We have used the same simulation Pythia Montecarlo data as before, as well as the same overall procedure (not the algorithm, evidently) for training and testing. A remarkable difference is that now we represent the physical observables by five decimal digit integers, against the double precision floating point representation needed for the backpropagation NN. The *truth* value for a Higgs event was fixed to 8192 and to 0 for a background events, while the threshold parameter controlling the purity level was varied by steps of unity between the two *truth* values. The results in terms of purity and efficiency are collected in Fig. 2 for a case of 8-bit synaptic weights and 200 GeV of Higgs mass (the data are represented by stars).

4 Conclusions

Neural networks have a clear advantage over traditional statistical methods, since they can support a high degree of parallelism and could be used for on-line analysis of the experimental data. Therefore their use in the future LHC experiments should be seriously considered and thoroughly investigated. We have contributed to this analysis by considering two different nets. The first one is a simulated ANN trained by the backpropagation algorithm. The second one is a hardware implementation of a fast NN, the neurochip TOTEM.

Our results show that NN can be helpful in the discrimination of background events from the signal in the Higgs search at the future Large Hadron Collider to be built at CERN. We have proved this by considering one particular Higgs decay channel ($H \rightarrow 4\mu$) in the mass range $M_H \in (150 - 200)$ GeV and including the most relevant backgrounds: $t\bar{t}$ and $Zb\bar{b}$. For both the neural nets, the case $M_H \simeq 200$ GeV is more favourable, and acceptable values of purity and efficiency can be obtained; in particular the neural chip TOTEM produces in general better performances and, in view of its possible on-line implementation, should be seriously considered, in our opinion, as a tool for the analyses to be performed at the future Large Hadron Collider at Cern.

Acknowledgments. We wish to thank G. Marchesini for most useful comments and P. De Felice and G. Pasquariello for their collaboration at an early stage of this work.

⁴For a comparison in performance between TOTEM and backpropagation based neurochips see for instance [23]

References

- [1] R. Casalbuoni, S. De Curtis, D. Dominici and R. Gatto, Nucl. Phys. **B 282** (1987) 235; R. Casalbuoni, P. Chiappetta, D. Dominici, F. Feruglio and R. Gatto, Phys. Lett. **B 269** (1991) 361.
- [2] D. Froidevaux, in Proc. of *Large Hadron Collider Workshop*, Eds. G. Jarlskog and D. Rein, CERN 90-10 and ECFA 90-133, Vol. II, pag. 444; A. Nisati, ibid. pag. 492; M. Della Negra et al., ibid. pag. 509.
- [3] J. Hertz, A. Krogh and R. G. Palmer, *Introduction to the Theory of Neural Computation* (Addison-Wesley) (1991).
- [4] L. Lönnblad, C. Petersen and T. Rönvaldsson, Phys. Rev. Lett. **65** (1990) 1321.
- [5] L. Lönnblad, C. Petersen and T. Rönvaldsson, Nucl. Phys. **B 349** (1991) 675; C. Bortolotto, A. De Angelis and L. Lanceri, Nucl. Inst. and Methods **A 306** (1991) 457; L. Bellantoni et al., Nucl. Inst. and Methods **A 310** (1991) 618.
- [6] G. Marchesini, G. Nardulli and G. Pasquariello, Nucl. Phys. **B 394** (1993) 541.
- [7] P. Chiappetta, P. Colangelo, P. DeFelice, G. Nardulli and G. Pasquariello, Phys. Lett. **B 322** (1994) 219.
- [8] F. Anselmo et al., Nuovo Cim. **107 A** (1994) 129.
- [9] C. Bortolotto, A. de Angelis, N. D. Groot and J. Seixas, Int. Journ. of Modern Physics **C 3** (1992) 733.
- [10] P. Mazzanti and R. Odorico, Int. Jour. of Neural Systems **3** (1992) 243.
- [11] B. Denby, *The use of Neural Networks in High Energy Physics*, in Neural Computation **4** (5) (1993) 505.
- [12] D. E. Rumelhart, G. E. Hinton and R. J. Williams, in *Parallel Distributed Processing: Explorations in the Microstructure of Cognition*, MIT Press, Cambridge MA (1986).
- [13] G. Anzellotti et al., Journ. of Mod. Phys. C, **6** (1995) 555
- [14] R. Battiti and G. Tecchiolli, *The Reactive Tabu Search*, ORSA Journal on Computing, **6** (2) (1994) 126.
- [15] R. Battiti and G. Tecchiolli, “*Training Neural Nets with the Reactive Tabu Search*”, IEEE Transactions on Neural Networks, **6** (1995) 1185.
- [16] ALEPH Collab., Phys. Lett. **B 313** (1993) 299.
- [17] M. Luscher and P. Weisz Nucl. Phys. **B 290** (1987) 5; **B 295** (1988) 65 and **B 318** (1989) 705.
- [18] M. Mangano and T. Trippe of the Particle Data Group, in *Review of Particle Properties*, Phys. Rev. **D 54** (1996) 309.
- [19] H. U. Bengtsson and T. Sjöstrand, Computer Physics Commun. **46** (1987) 43; T. Sjöstrand, CERN-TH.6488/92.

- [20] S. Catani, Yu. L. Dokshitzer, M. Olsson, G. Turnock and B. R. Webber, Phys. Lett. **B 269** (1991) 432; S. Bethke, Z. Kunszt, D. E. Soper and W. J. Stirling, Nucl. Phys. **B 370** (1992) 310; N. Brown and W. J. Stirling, Zeit. Phys. **C 53** (1992) 629. Yu. L. Dokshitzer and M. Olsson, Nuc. Phys. **B 396** (1993) 137.
- [21] S. Catani, in Proc. of *Int. Europhysics Conf. on High Energy Physics, Marseille 1993*, eds. J. Carr and M. Perrottet (Ed. Frontieres, France) (1994) 771.
- [22] P. De Felice, G. Nardulli and G. Pasquariello, Phys. Lett. **B 354** (1995) 473.
- [23] C.S. Lindsey and Th. Linblad, “Experience with RTS as implemented in the TOTEM chip”, *Proc. of ICNN96*, Washington D.C., June 1996.

FIGURE CAPTIONS

Fig. 1

X_{10} distribution for, from the left, Higgs signal, $t\bar{t}$ and $Zb\bar{b}$ background.

Fig. 2

The purity P versus the Higgs efficiency η for two different NN in the case $M_H = 200$ GeV.

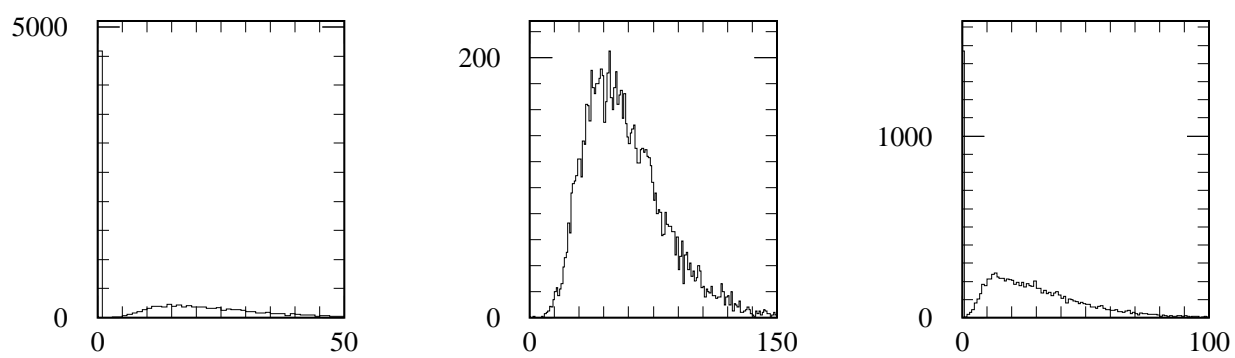


Fig.1

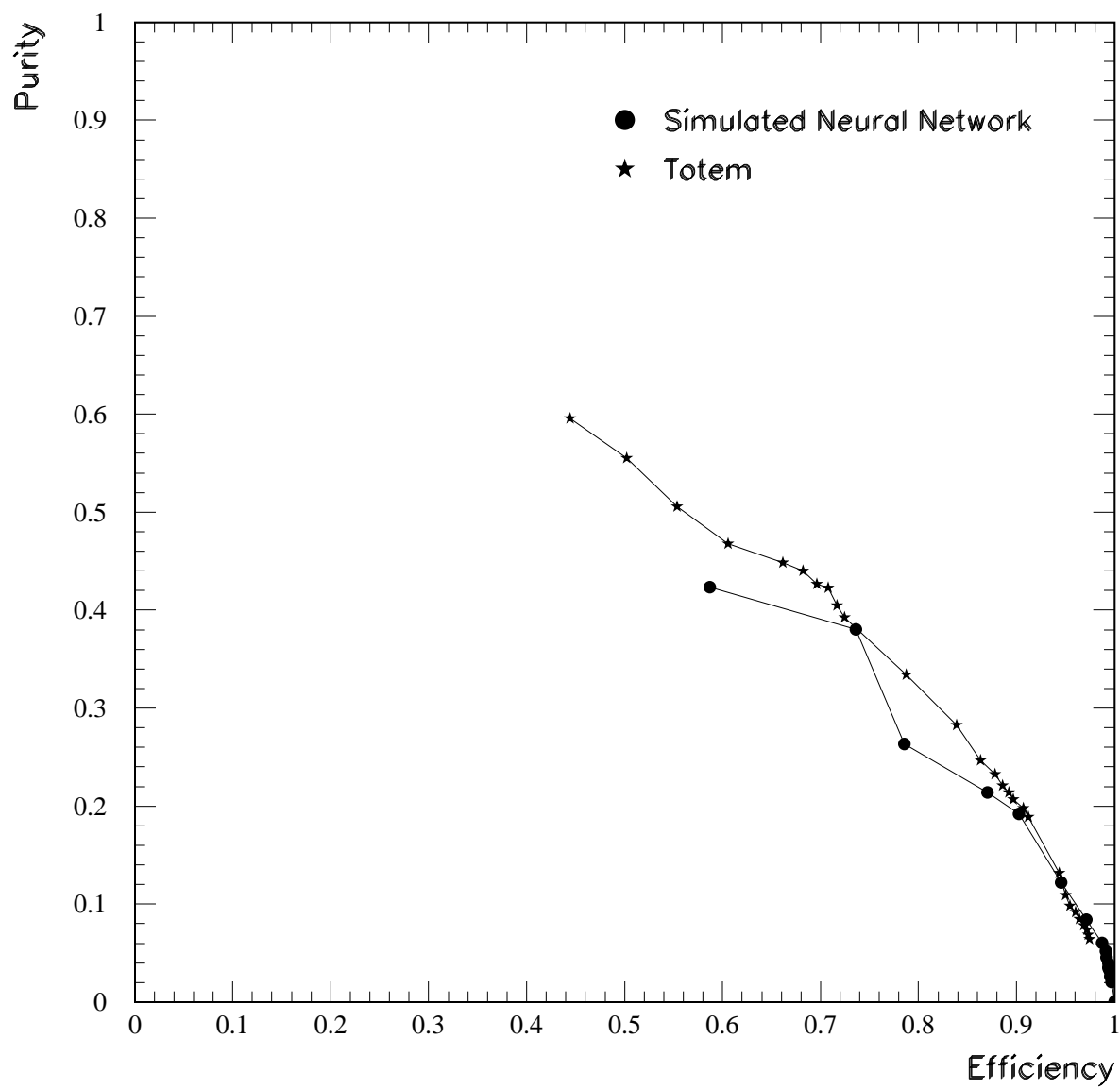


Fig.2